

# Mat1062: Introductory Numerical Methods for PDE

Mary Pugh

March 5, 2009

## 1 Ownership

These notes are the joint property of Rob Almgren and Mary Pugh.

## 2 Examples of consistent, conservative schemes

From before, we have four finite-difference schemes for the linear advection equation: explicit upwind, Lax-Friedrichs, Lax-Wendroff, and Beam-Warming. They work well for the advection equation and so a natural question is “Can they be generalised to nonlinear conservation laws?”

Note that for the advection equation  $u_t + au_x = 0$  we write this in conservative form  $u_t + (f(u))_x = 0$  where  $f(u) = au$ .

**Explicit Upwind** For  $u_t + au_x = 0$ , if  $a > 0$  the scheme is

$$u_j^{n+1} = u_j^n - \frac{ak}{h} (u_j^n - u_{j-1}^n) = u_j^n - \frac{k}{h} (f(u_j^n) - f(u_{j-1}^n))$$

and if  $a < 0$  the scheme is

$$u_j^{n+1} = u_j^n - \frac{ak}{h} (u_{j+1}^n - u_j^n) = u_j^n - \frac{k}{h} (f(u_{j+1}^n) - f(u_j^n))$$

We seek a flux function  $F(u_L, u_R)$  so that this scheme can be written as

$$u_j^{n+1} = u_j^n - \frac{k}{h} \left( F(u_{j+1}^n, u_j^n) - F(u_j^n, u_{j-1}^n) \right),$$

If we have a smooth solution of  $u_t + (f(u))_x = u_t + f'(u)u_x = 0$  then we see that the direction that the characteristic is moving will be determined

by the sign of  $f'(u)$ . This sign then determines which of the above upwind schemes we would want to use. For this reason, we take

$$F(u_L, u_R) = \begin{cases} f(u_L) & \text{if } \frac{f(u_R) - f(u_L)}{u_R - u_L} \geq 0 \\ f(u_L) & \text{if } u_L = u_R \\ f(u_R) & \text{if } \frac{f(u_R) - f(u_L)}{u_R - u_L} < 0 \end{cases} \quad (1)$$

We now check if this will result in a consistent scheme. By construction,  $F(\bar{u}, \bar{u}) = f(\bar{u})$  for all  $\bar{u} \in \mathbb{R}$ . It remains to check the Lipschitz continuity requirement. This will follow if  $f$  is Lipschitz continuous.

$$\begin{aligned} |F(u_L, u_R) - f(\bar{u})| &= \begin{cases} |f(u_L) - f(\bar{u})| \\ |f(u_R) - f(\bar{u})| \end{cases} \\ &\leq \begin{cases} K|u_L - \bar{u}| \\ K|u_R - \bar{u}| \end{cases} \leq K \max\{|u_L - \bar{u}|, |u_R - \bar{u}|\} \end{aligned}$$

Above, I used a short-hand: for the “cases” notation, I didn’t bother to write down which situation led to what since it doesn’t actually matter in finding the desired upper bound.

Here’s another way to have understood how the flux function  $F(u_L, u_R)$  was chosen. We are trying to approximate the time average of the flux across  $x = x_{j+1/2}$ :

$$F_{j+1/2}^n = \frac{1}{k} \int_{t_n}^{t_{n+1}} f(u(x_{j+1/2}, t)) dt.$$

The crudest approximation would be to approximate the integrand with a constant:

$$f(u(x_{j+1/2}, t)) \approx f(u(x_{j+1/2}, t_n))$$

which would yield

$$F_{j+1/2}^n = \frac{1}{k} \int_{t_n}^{t_{n+1}} f(u(x_{j+1/2}, t)) dt \approx f(u(x_{j+1/2}, t_n)).$$

Now there’s the question of “we want the flux at  $x_{j+1/2}$  at time  $t_n$  and all we have are the cell averages over  $[x_{j-1/2}, x_{j+1/2}]$  and  $[x_{j+1/2}, x_{j+3/2}]$  at time  $t_n$ ...” The answer is to bear in mind the direction of flow: if  $f_u(u(x_{j+1/2}, t)) > 0$  then we take the flux based on the cell average to the left and  $F_{j+1/2}^n \approx f(u_L)$ . If  $f_u(u(x_{j+1/2}, t)) < 0$  then we take the flux based on the cell average to the right and  $F_{j+1/2}^n \approx f(u_R)$ . This is precisely the numerical flux  $F(u_L, u_R)$  described by (1).

**Lax-Friedrichs** For  $u_t + au_x = 0$ , we had

$$\begin{aligned} u_j^{n+1} - u_j^n &= -\frac{\mu}{2}(u_{j+1}^n - u_{j-1}^n) + \frac{1}{2}(u_{j-1}^n - 2u_j^n + u_{j+1}^n) \\ &= -\frac{k}{h} \left( \left[ \frac{a}{2}(u_{j+1}^n + u_j^n) - \frac{h}{2k}(u_{j+1}^n - u_j^n) \right] \right. \\ &\quad \left. - \left[ \frac{a}{2}(u_j^n + u_{j-1}^n) - \frac{h}{2k}(u_j^n - u_{j-1}^n) \right] \right) \end{aligned}$$

from which we identify the linear flux function

$$F_{\text{linear}}(u_L, u_R) = \frac{a}{2}(u_R + u_L) - \frac{h}{2k}(u_R - u_L).$$

And so, the nonlinear analog should be

$$F(u_L, u_R) = \frac{f(u_R) + f(u_L)}{2} - \frac{h^2}{2k} \frac{u_R - u_L}{h}. \quad (2)$$

That is, we just average  $f(u)$  from both sides, and add a pure diffusive flux with  $D = h^2/2k \sim \mathcal{O}(h)$ , since  $u_t = Du_{xx}$  effectively has  $f = -Du_x$ . (In fact, the averaging of  $f(u)$  also has a small diffusive effect, which is why we had a factor  $1 - \mu$  in the linear analysis.)

We now check the consistency. First, does  $F$  agree on the diagonal?

$$F(\bar{u}, \bar{u}) = \frac{f(\bar{u}) + f(\bar{u})}{2} - \frac{h^2}{2k} \frac{\bar{u} - \bar{u}}{h} = f(\bar{u})$$

as desired. Now we check the Lipschitz continuity:

$$\begin{aligned} |F(u_L, u_R) - F(\bar{u}, \bar{u})| &\leq \left| \frac{f(u_R) - f(\bar{u})}{2} \right| + \left| \frac{f(u_L) + f(\bar{u})}{2} \right| \\ &\quad + \frac{h}{2k} |u_R - \bar{u}| + \frac{h}{2k} |u_L - \bar{u}|. \end{aligned}$$

This shows that if  $f$  is Lipschitz continuous then  $F$  will be as well. Therefore if the scheme is converging to something, the limit will be a weak solution. (Note: in practice, you can't show convergence on a computer. What you can do is compute a few refinements and find the differences between the refinements and see if the errors are decreasing in  $L^1$ . If they appear to be decreasing with a well-defined rate then it's plausible that the solutions are converging to something. But it's not a proof.)

From our stability analysis of the linear advection problem, we expect that this method will slightly smear discontinuities, but not introduce any oscillations.

**Lax-Wendroff** For  $u_t + au_x = 0$ , we have

$$\begin{aligned} u_j^{n+1} - u_j^n &= -\frac{\mu}{2}(u_{j+1}^n - u_{j-1}^n) + \frac{\mu^2}{2}(u_{j-1}^n - 2u_j^n + u_{j+1}^n) \\ &= -\frac{k}{h} \left( \left[ \frac{a}{2}(u_{j+1}^n + u_j^n) - \frac{a^2k}{2h}(u_{j+1}^n - u_j^n) \right] \right. \\ &\quad \left. - \left[ \frac{a}{2}(u_j^n + u_{j-1}^n) - \frac{a^2k}{2h}(u_j^n - u_{j-1}^n) \right] \right) \end{aligned}$$

so the linear flux is

$$F_{\text{linear}}(u_L, u_R) = \frac{a}{2}(u_R + u_L) - \frac{a^2k}{2h}(u_R - u_L).$$

The first term is the same as for Lax-Friedrichs, but the second term is a little more challenging. We identify  $au \mapsto f(u)$ , and as above, we don't mind having left-over factors of  $u$  with no  $a$ , but what do we do with the extra factor of  $a$ ? Answer: we write the nonlinear flux as

$$F(u_L, u_R) = \frac{f(u_R) + f(u_L)}{2} - \frac{k}{2h} A(u_L, u_R) (f(u_R) - f(u_L)) \quad (3)$$

where  $A(u_L, u_R)$  is an approximation to  $df/du$  at the cell boundary. A typical choice would be

$$A(u_L, u_R) = \frac{df}{du}(u_{\text{mid}}) \quad \text{where} \quad u_{\text{mid}} = \frac{u_L + u_R}{2}.$$

Note that if we were computing a system of conservation laws then  $A(u_L, u_R)$  would be the Jacobian of  $\vec{f}(\vec{u})$  evaluated at a state between  $\vec{u}_L$  and  $\vec{u}_R$ . Evaluating this Jacobian can be computationally expensive, so there are alternative schemes to avoid it. From our experience in the linear problem, we expect this scheme to introduce oscillations.

Like for the explicit upwind method, there's another way to understand how the flux function  $F(u_L, u_R)$  was chosen. We are trying to approximate

$$F_{j+1/2}^n = \frac{1}{k} \int_{t_n}^{t_{n+1}} f(u(x_{j+1/2}, t)) dt$$

for example. The crudest approximation would be to approximate the integrand with something piecewise linear in time:

$$f(u(x_{j+1/2}, t)) \approx f_0 + f_1(t - t_n). \quad (4)$$

This would yield

$$F_{j+1/2}^n = \frac{1}{k} \int_{t_n}^{t_{n+1}} f(u(x_{j+1/2}, t)) dt \approx f_0 + \frac{f_1}{2}k.$$

What is the piecewise linear function to take? Do a Taylor series expansion in  $t$  of  $f(u(x_{j+1/2}, t))$ :

$$\begin{aligned} f(u(x_{j+1/2}, t)) &\approx f(u(x_{j+1/2}, t_n)) + f_u(u(x_{j+1/2}, t_n)) u_t(x_{j+1/2}, t_n) (t - t_n) \\ &= f(u(x_{j+1/2}, t_n)) + f_u(u(x_{j+1/2}, t_n)) (f(u(x, t_n)))_x|_{x=x_{j+1/2}} (t - t_n) \\ &\approx \frac{f(u_L) + f(u_R)}{2} + f_u(u_{\text{mid}}) \frac{f(u_R) - f(u_L)}{h} (t - t_n) \end{aligned}$$

where  $u_{\text{mid}} = (u_L + u_R)/2$ . Using this in (4) yields

$$F(u_L, u_R) = \frac{f(u_L) + f(u_R)}{2} + \frac{k}{2} f_u(u_{\text{mid}}) \frac{f(u_R) - f(u_L)}{h}$$

which is precisely (3). From the above derivation, we see that the numerical flux

$$F(u_L, u_R) = f(u_{\text{mid}}) + \frac{k}{2} f_u(u_{\text{mid}}) \frac{f(u_R) - f(u_L)}{h}$$

would have been equally natural.

We have only touched the surface of numerical methods for conservation laws. There are many more sophisticated methods, mostly based on using explicit local solutions of the nonlinear problem near the cell walls and then either averaging the result (“Godunov” methods) or sampling it (Glimm’s method). Multidimensional problems pose a whole new set of challenges.

### 3 Conservative schemes in action

We consider the conservation law  $u_t + (1/2 u^2)_x = 0$  with initial data  $u_0(x) = (1 - \tanh(3x))/2$  on  $[-\pi, \pi]$ . This is a monotonic profile that is very close to 1 at  $x = -\pi$  and very close to 0 at  $x = \pi$ .

We compute solutions using the three schemes presented in the March 6 notes: the nonlinear analogues of the explicit upwind scheme, the Lax-Friedrichs scheme, and the Lax-Wendroff scheme. We have certain expectations from how these schemes perform for the linear advection equation:

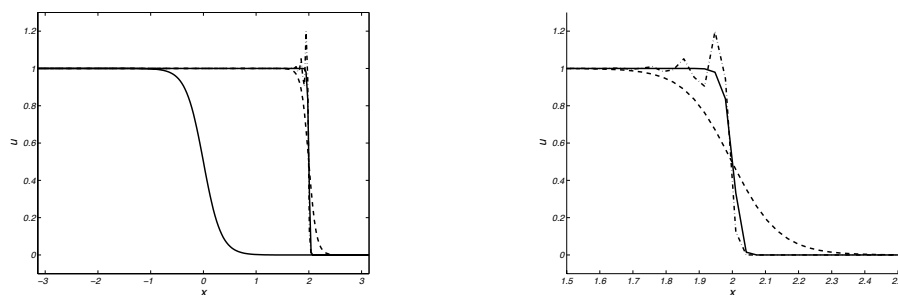


Figure 1: The solutions are computed on  $[-\pi, \pi]$  with time-step  $k = 4/300$  and space-step  $h = \pi/100$ . In both plots: solid line: explicit upwind; dashed line: Lax-Friedrichs; dot-dash line: Lax-Wendroff. Left plot: the solid line to the left of the others is the initial data. The other three curves represent the approximate solutions at time  $t = 4$ . Right plot: a close-up near the “shock region”.

we expect the schemes inspired by the explicit upwind and Lax-Friedrichs schemes to be dissipative and the scheme inspired by the Lax-Wendroff scheme to be dispersive.

In the left plot of Figure 1, you see the initial data, along with the three approximate solutions at time  $t = 4$ . All three of the approximate solutions are markedly steeper than they were at time  $t = 0$ . In the right plot of Figure 1, you see a close-up of the “shock region”. As expected, the Lax-Wendroff solution has dispersive ripples behind the advancing front while both the explicit upwind and Lax-Friedrichs solution have monotonic profiles. The Lax-Wendroff solution has markedly more smoothing of the “shock region”.

Because the schemes all have numerical dissipation or numerical dispersion, the approximate solutions will never actually shock. The slopes in the “shock region” are steep and become steeper the smaller  $h$  and  $k$  are. However, they cannot go to  $-\infty$  in finite time (the solution cannot shock). That said, we want to know if these shock regions are moving with the desired speed. To test this, at each moment in time  $t_n$ , for each profile we find a point  $\xi(t)$  at which the approximate solution equals  $1/2$ . In figure 2 we plot these points in the  $x$ - $t$  plane, one curve for each of the three computed solutions. On the large scale, shown in the left plot, the three shocks coincide and appear to have the correct speed — the curves start at  $(0, 0)$  and end at  $(2, 4)$  which is consistent with the exact solution whose shock moves with speed  $\xi'(t) = 1/2$ . On the small scale, shown in the right plot, we see that for the explicit upwind scheme and the Lax-Wendroff scheme the speed of

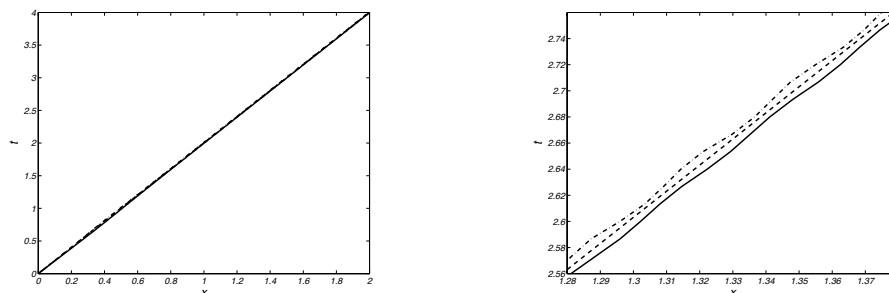


Figure 2: At a given time  $t_n$  we find  $j$  so that  $u_{j-2}^n, u_{j-1}^n, u_j^n \geq 1/2$  and  $u_{j+1}^n, u_{j+2}^n, u_{j+3}^n < 1/2$ . We then do spline interpolation based on these six points on the graph  $(x_{j-2}, u_{j-2}^n), \dots, (x_{j+3}, u_{j+3}^n)$ . We then use the interpolating polynomial to find the location  $\xi(t_n)$  at which the interpolating polynomial equals  $1/2$ . We do this for the three approximate solutions, computed by the three schemes. As before, in both plots: solid line: explicit upwind; dashed line: Lax-Friedrichs; dot-dash line: Lax-Wendroff. Left plot: we plot  $(\xi(t), t)$  for the three solutions. Right plot: a close-up of the left plot.

$\xi(t)$  is slightly oscillatory relative to the Lax-Friedrichs scheme. On average, however, there is no great effect — if we approximate  $\xi'(t)$  and ask for the average over the time-window  $[2, 4]$  then the explicit upwind scheme has an average speed of 0.49979, the Lax-Friedrichs scheme has an average speed of 0.50022, and the Lax-Wendroff scheme has an average speed of 0.49995.

## 4 Rates of Convergence

Let's check the rates of convergence. I consider solutions of  $u_t + (u^2/2)_x = 0$  computed using the Lax-Wendroff scheme with initial data

$$u_0 = \frac{1 - \tanh(10x)}{2}$$

on  $(-\pi, \pi)$ . The boundary conditions are taken as  $u(-\pi, t) = 1$  and  $u(\pi, t) = 0$  for  $t > 0$ .

First, I compute up to time  $T = .1$  using the space step  $h = 2\pi/100$  and time step  $k = T/100$ . Then I compute the solution using  $h/2$  and  $k/2$  and so on. In this way, I compute eight solutions. I was too lazy to code in the exact solution at  $t = .1$  to compare to the approximate solutions at  $t = .1$ , instead I computed the  $L^1$  norm of the successive differences:

	L <sup>1</sup> norm	ratio
$\ u_1 - u_2\ _{L^1}$	6.6303e-03	3.0591
$\ u_2 - u_3\ _{L^1}$	2.1674e-03	3.4514
$\ u_3 - u_4\ _{L^1}$	6.2798e-04	3.8828
$\ u_4 - u_5\ _{L^1}$	1.6173e-04	3.9466
$\ u_5 - u_6\ _{L^1}$	4.0980e-05	3.9880
$\ u_6 - u_7\ _{L^1}$	1.0276e-05	3.9954
$\ u_7 - u_8\ _{L^1}$	2.5719e-06	

In this way, we see that before the shock time, the scheme has the expected  $\mathcal{O}(h^2, k^2)$  convergence rate.

Now, I compute up to a time after the shock time. Specifically, I compute up to time  $T = .6$  using the space step  $h = 2\pi/100$  and time step  $k = T/600$ . Then I compute the solution using  $h/2$  and  $k/2$  and so on. In this way, I compute eight solutions, with precisely the same values of  $h$  and  $k$  as before. As above, I compute the L<sup>1</sup> norm of the successive differences at time  $T = .6$ :

	L <sup>1</sup> norm	ratio
$\ u_1 - u_2\ _{L^1}$	1.6376e-01	1.2987
$\ u_2 - u_3\ _{L^1}$	1.2609e-01	1.1812
$\ u_3 - u_4\ _{L^1}$	1.0674e-01	1.1624
$\ u_4 - u_5\ _{L^1}$	9.1827e-02	1.4122
$\ u_5 - u_6\ _{L^1}$	6.5023e-02	1.5429
$\ u_6 - u_7\ _{L^1}$	4.2144e-02	1.9148
$\ u_7 - u_8\ _{L^1}$	2.2009e-02	

The convergence rate is markedly slower. Admittedly, the ratios are increasing and one might imagine that once the values of  $h$  and  $k$  were small enough for the differences to be on the order of  $1e - 06$  (as for the  $T = .1$  case) then perhaps the scheme would be converging at the rate of  $\mathcal{O}(h^2, k^2)$ . However, I am not inclined to believe this is the case. We know that after a finite time the solution becomes a piecewise constant weak solution. Earlier, we considered the convergence rates for the different schemes applied to the linear PDE  $u_t + au_x = 0$ . There, we saw a reduced rate of convergence for such weak solutions. The nonlinear PDE is effectively a linear PDE when applied to a piecewise constant solution (since  $f_u(u)$  will be constant almost everywhere) and so I expect that we have the exact same type of reduced convergence rate as we saw before.

## 5 A Cautionary Tale

We now consider the explicit upwind scheme. We take two choices for initial data:

$$u_0(x) = \begin{cases} -1 & \text{if } x < 0 \\ 0 & \text{if } x = 0, \\ 1 & \text{if } x > 0 \end{cases}, \quad v_0(x) = \begin{cases} -1 & \text{if } x \leq 0 \\ 1 & \text{if } x > 0 \end{cases},$$

When choosing the discretization for this initial data, I made sure that there was a mesh-point at  $x = 0$  so that

$$u_j^0 = \begin{cases} -1 & \text{if } j < 0 \\ 0 & \text{if } j = 0, \\ 1 & \text{if } j > 0 \end{cases}, \quad v_j^0 = \begin{cases} -1 & \text{if } j \leq 0 \\ 1 & \text{if } j > 0 \end{cases}. \quad (5)$$

If I had not done this then the initial data for the approximate scheme would have been indistinguishable from one another. In the left plot of Figure 3 I present the approximate solution  $u$  at a sequence of times  $t = 0, 1/4, 2/4, \dots, 8/4$ . We see that the jump discontinuity instantaneously replaced by a continuous function and that as time passes the slope at  $x = 0$  is a positive decreasing function. In fact,  $v$  is a *rarefaction wave* which is something we'll study shortly. In the right plot of 3 we present the solutions  $u$  and  $v$  both at time  $t = 1$ . Interestingly, we see that  $v$  hasn't changed:  $v_j^n = v_j^0$  for all  $n$  and all  $j$ . This is striking because  $v_0(x)$  and  $u_0(x)$  agree at all points except at  $x = 0$ . Indeed, the value at  $x = 0$  has a massive effect on the resulting solution. Both  $u$  and  $v$  are valid weak solutions of  $u_t + (1/2 u^2)_x = 0$ . However,  $u$  is the physically desirable one: it satisfies the "entropy condition".

Finally, we note that the initial data  $v_j^0$  is not consistent with cell averages. Given  $v(x)$ , the average value over any interval centered at  $x = 0$  is 0, not 1. In general, if the initial data has a jump in it we need to put a meshpoint at the jump and use the value  $(u_L + u_R)/2$  in the initial data at that point.

## 6 Finite Volume Methods

The approach we took for the conservation laws is a case of the finite volume method. Specifically, rather than tracking values of  $u(x, t)$  at points in space

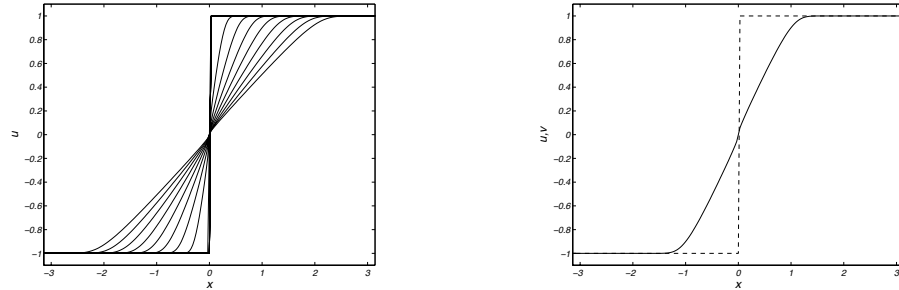


Figure 3: Solutions of  $u_t + (1/2 u^2)_x = 0$  using the initial data (5). The explicit upwind scheme is used with  $h = \pi/100$  and  $k = 1/100$ . Left plot: the approximate solution  $u$  is shown at times  $t = 0, 1/4, 2/4, \dots, 8/4$ . As time passes the central region expands and the derivative at  $x = 0$  decreases. Right plot: the approximate solution  $u$  (solid) and  $v$  (dashed) are shown at time  $t = 1$ . The solution  $v$  is stationary — it equals the initial data. The solution  $u$  has had its central region expand as shown in the plot to the left.

time, we tracked the average values of  $u$  over intervals in space. As a simple example of how one could use the finite volume method in a different context, we consider a diffusion equation

$$u_t = (D(x) u_x)_x \quad (6)$$

where the diffusion depends on space. We consider the PDE (6) on the interval  $[0, L]$ . We divide this interval up as usual, into  $N$  intervals of equal length. We denote the centers of these intervals by

$$x_j = jh - \frac{h}{2} \quad 1 \leq j \leq N.$$

The left-hand and right-hand endpoints of the intervals are

$$x_{j-1/2} = (j-1)h \quad \text{and} \quad x_{j+1/2} = jh$$

respectively. Note that the  $x_j$ 's are different from the ones that we've used up to now. The  $N$  cell averages are

$$u_j(t) = \frac{1}{h} \int_{x_{j-1/2}}^{x_{j+1/2}} u(x, t) dx \quad 1 \leq j \leq N$$

To find how these cell averages should evolve, we integrate the PDE (6) resulting in

$$\begin{aligned} \frac{d}{dt} \frac{1}{h} \int_{x_{j-1/2}}^{x_{j+1/2}} u(x, t) dx &= \frac{1}{h} \int_{x_{j-1/2}}^{x_{j+1/2}} u_t(x, t) dx = \frac{1}{h} \int_{x_{j-1/2}}^{x_{j+1/2}} (D(x) u_x)_x dx \\ &= \frac{1}{h} (D(x_{j+1/2}) u_x(x_{j+1/2}, t) - D(x_{j-1/2}) u_x(x_{j-1/2}, t)). \end{aligned}$$

Integrating this in time, we find

$$u_j^{n+1} = u_j^n + \frac{k}{h} \left( \frac{1}{k} \int_{t_n}^{t_{n+1}} D(x_{j+1/2}) u_x(x_{j+1/2}, t) dt - \frac{1}{k} \int_{t_n}^{t_{n+1}} D(x_{j-1/2}) u_x(x_{j-1/2}, t) dt \right). \quad (7)$$

We now see that we're in a similar situation as before: to compute the cell average at time  $t_{n+1}$  we need the cell average at time  $t_n$  as well as the time averages of the flux in and out of the cell across its boundaries.

How can we approximate the time averages of the flux in and out of the cell using the cell averages  $\{u_j\}$ ? One approach would be to approximate the derivative at the left-hand endpoint for times  $t \in [t_n, t_{n+1}]$  via the difference of the cell average to its right ( $u_j^n$ ) and the cell average to its left ( $u_{j-1}^n$ ):

$$u_x(x_j - h/2, t) \approx \frac{u_j^n - u_{j-1}^n}{h}.$$

This results in the time-average

$$\frac{1}{k} \int_{t_n}^{t_{n+1}} u_x(x_j - h/2, t) dx \approx \frac{1}{k} \frac{u_j^n - u_{j-1}^n}{h} k = \frac{u_j^n - u_{j-1}^n}{h}.$$

Using this approximation in (7) and assuming Neumann boundary conditions at the endpoints results in

$$\begin{aligned} u_1^{n+1} &= u_1^n + \frac{k}{h} D(x_{1+1/2}) \frac{u_2^n - u_1^n}{h}, \\ u_j^{n+1} &= u_j^n + \frac{k}{h} \left( D(x_{j+1/2}) \frac{u_{j+1}^n - u_j^n}{h} - D(x_{j-1/2}) \frac{u_j^n - u_{j-1}^n}{h} \right), \quad 2 \leq j \leq N-1 \\ u_N^{n+1} &= u_N^n - \frac{k}{h} D(x_{N-1/2}) \frac{u_N^n - u_{N-1}^n}{h}. \end{aligned} \quad (8)$$

Note that I was lucky to have boundary conditions at  $x = 0, L$  that involved prescribing a flux  $u_x(0, t)$  and  $u_x(L, t)$ . If I'd had other boundary conditions then I would have had to think carefully about how to approximate the time averages of the flux in at  $x = 0$  and out at  $x = L$ .

The time-stepping scheme (8) looks precisely like the Explicit Euler finite difference scheme! In fact, it is. How should we understand this?

- The finite difference approach and the finite volume approach have different initial data (samples versus averages) and the approximate solutions are plotted differently (points versus a piecewise constant function) and interpreted differently (samples versus averages).
- By construction, the finite volume method has a chance of converging to a weak solution, because it's based on the integral formulation ((7), for example). But we've already seen via conservation laws that whether or not the limiting object (if it exists) is a weak solution will depend on how the fluxes were approximated.
- Just as there are other finite-difference approximations of  $u_{xx}$  than the three-point centered one, there are other ways to approximate the time-averages of the fluxes. And so it's not inevitable that all finite volume discretizations are the same as some finite difference approximation and vice versa.
- By taking a finite volume approach when considering an equation which is a conservation law or has a divergence structure to it ( $u_t = \nabla \cdot (D(x)\nabla u)$ , for example) the physics that was used in deriving the PDE is naturally enforced. (This is because the derivation of such PDEs is done by: integrating the quantity of interest over an arbitrary region in space, figuring out how that integral evolves in time (resulting in an integral formulation of the problem), assuming that the quantity of interest is smooth (not always a valid assumption), and then deducing the PDE.)

For more about finite volume methods, I recommend the book "Finite-volume methods for hyperbolic problems" by R. J. LeVeque. It's in the engineering library and the math/stat library, call number QA 377 .L41566.